



Enhanced delineation of reservoir compartmentalization from advanced Pre and Post-stack seismic attribute analysis

Mauricio Herrera Volcan

Schlumberger
256 St Georges Tce, Perth, 6000, WA, Australia

MVolcan@slb.com

Clark Chahine

Schlumberger
CChahine@slb.com

Leigh TrueLove

Schlumberger
LTruelove@slb.com

SUMMARY

Reservoir compartmentalization has a huge bearing on fluid flow within hydrocarbon reservoirs, and can impact overall recovery during field development. Small and sub-seismic faults can have a dramatic effect on the compartmentalization within a reservoir, but until recently they have not typically been incorporated into fault interpretations. This can be due to data fidelity and the amount of time needed to manually pick them. Their omission from the interpretation – and ultimately reservoir models – means the understanding of reservoir compartmentalization is incomplete, hence solving this problem is critical to improve production. Approaches that automatically identify and extract faults from seismic volumes are available. These automated methods aim to emphasize discontinuities within seismic volumes and are usually focused on poststack data. However, they need preconditioned inputs that are often based around a coherence algorithm. This preconditioning aims to suppress noise but can inflict data degradation, which may diminish smaller features in the seismic volumes. This article proposes an enhanced approach using a new combination of preconditioning steps designed to avoid these degradation problems. It also proposes the use of prestack seismic data, which has not traditionally been used for this purpose. Analysis of various pre-stack elements is displayed to show it can delineate more features than poststack data alone in certain noisy areas, such as gas effects or low frequencies. Finally, it demonstrates that the best approach combines results from pre- and poststack analysis to produce a more complete picture of reservoir compartmentalization.

INTRODUCTION

Background

Reliable automated identification of faults in seismic data would dramatically improve geophysical interpreters' productivity and significantly reduce the time needed to construct fault interpretations. A number of automated fault identification approaches have been attempted, but they are still not widely used due to a lack of consistency in the results, compared to an experienced geophysical interpreter. Poststack seismic data has until recently, been the primary input for seismic

interpretation, because prestack data has not been widely available or used in the exploration and development stages of subsurface modelling. Typical seismic fault identification approaches for pre- and post-stack data use various algorithms to manipulate and extract possible amplitude discontinuities typically associated with faults. Seismic data features can be accentuated or suppressed depending on the processing technique used. Interrogation of the original pre-stack gathers means these features may be observed and incorporated in the final analysis.

Amplitude data is frequently subject to signal degradation, which can be attributed to acquisition and processing techniques. This means that discontinuities can often be masked by these problems in the seismic volumes which makes identification difficult. As a result, there is a need to reduce, or smooth-out, the level of noise in the original amplitude data so discontinuities are made more obvious (Figure 1). There is considerable published material on the topics of noise removal including the application of Gaussian or anisotropic filtering, and coherence and variance attributes. Please refer to the following papers: Bahorich and Farner 1995, 1996; Fehmers and Hocker, 2002, 2003; Gersztenkorn and Marfurt, 1996a, 1996b; Gersztenkorn et al., 1999; Hesthammer, 1999; Iske and Randen 2005; Kirilin, 1992; Lees, 1999; Marfurt et al., 1999; Neff et al., 2000; Randen et al., 2000; van Bemmelen et al., 2000.

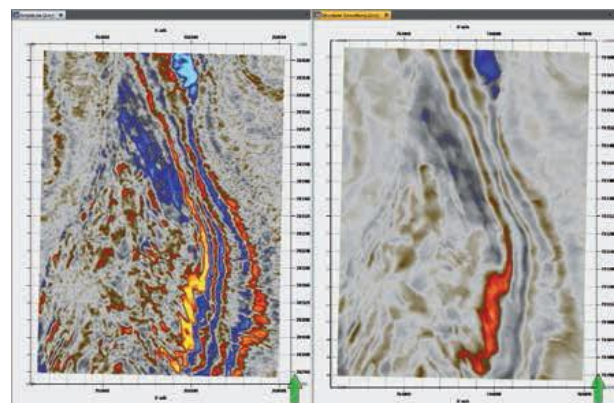


Figure 1 Comparison between raw SEGY and 'classic' seismic attributes designed to highlight amplitude discontinuities.

METHOD AND RESULTS

Amplitude contrast: a new approach to fault delineation
Traditional structure-oriented approaches that are designed to highlight the data within seismic volumes are still limited by the amount of signal-to-noise in the original amplitude data. As a result, attributes designed to suppress noise, such as structural smoothing (Figure 2), coherence (Bahorich and Farmer, 1995) or variance (Figure 1; van Bemmelen et al., 2000) remove noise but also remove data. These attributes create structural features that are more prominent and suppress noise in the resulting seismic volume; but often with a loss in fine scale detail. Understanding the distribution of these fine details, such as sub-seismic faults is critical to understanding reservoir flow pathways. Without a complete understanding of these small faults it is very difficult to understand the fluid flow in the reservoir. Classic noise suppression techniques may lead to these small features being removed, so they cannot be part of the final interpretation.

A different approach is to focus on these smaller faults, relying on larger faults being identified by classic methods (such as coherence and variance). Seismic surveys have inlines that are aligned perpendicular to the strike direction of major tectonic events. This means that the majority of larger structural features within the area of interest should be illuminated in the amplitude data and identifiable using traditional interpretation methods. Amplitude contrast has been applied as an alternative preprocessing step (to coherence *et al.*) prior to automatic fault extraction approaches (Figure 2). This methodology demonstrates considerable improvements in fault detection in comparison to classic methods such as coherence and variance (Figures 1 and 3; Aqrabi and Boe, 2011; Aqrabi et al., 2012). The amplitude contrast algorithm is loosely based on a Sobel filter (Gonzales and Woods, 2002) which performs a 2D spatial gradient measurement on an image, emphasizing regions of high spatial frequency which correspond to edges within the image. It has been used for many 2D and 3D seismic analyses, mainly to identify salt structures (Zhou, et al. 2007).

Comparison between amplitude contrast and variance (Figure 3) shows equivalent features that are identified between the two seismic attributes, but there is more resolution in the detection of fault-discontinuities by the amplitude contrast volume. Aqrabi and Boe (2011) show that the amplitude contrast methodology is much better at detecting faults within volumes along with highlighting significant signal-to-noise ratio. Classic methods, such as variance, have a good rate of success at discontinuity identification (Figure 2), but often suffer from these discontinuities being 'patchy' and lack the continuity needed to completely delineate the whole fault automatically (Figure 3). In comparison, the amplitude contrast results show more consistency and subsequently are better detected by the automated fault identification algorithms (Figure 3).

Combining amplitude contrast with edge evidence

Aqrabi et al., (2012) outline an approach which takes the results of the amplitude contrast and uses them as an input into automated fault extraction. They show the significant improvement to automated fault detection in comparison to variance-based approaches. This article proposes an extension to this approach by introducing an 'edge evidence'

intermediate step, to aid the automated fault identification algorithm (Figure 2).

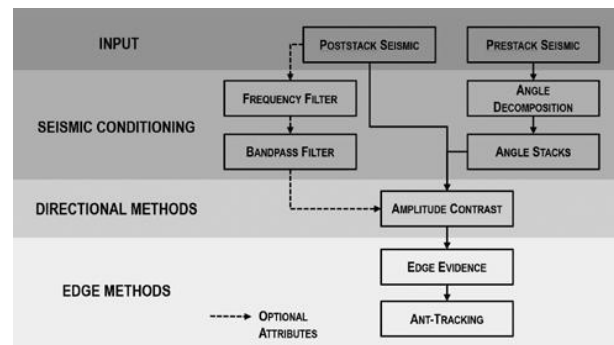


Figure 2 Standardised flow diagram showing automated fault extraction algorithm steps.

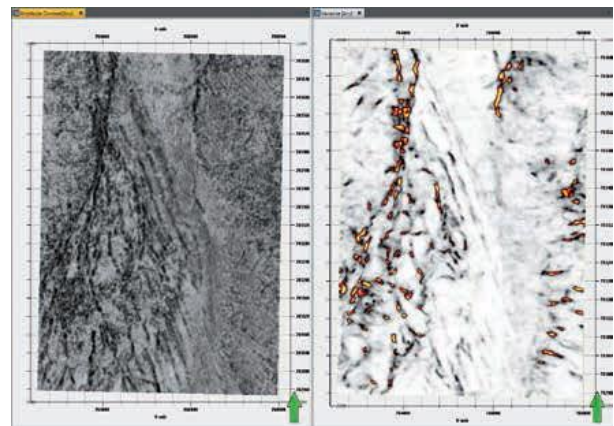


Figure 3 Comparison between variance and amplitude contrast showing the increased continuity of faults in the amplitude contrast volume.

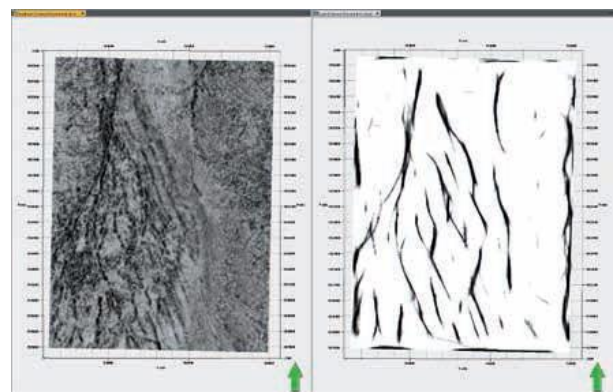


Figure 4 Result of edge evidence computed from amplitude contrast.

Edge evidence is a statistical edge enhancement method used to delineate fault and salt body borders within seismic data, and can be used when automated fault identification algorithms are struggling (Aqrabi and Boe, 2011). The algorithm is related to the Radon transform (Radon, 1917) and Hough transforms (Hough, 1959; Duda and Hart, 1972); but uses an integral to detect edges within an image, and is limited to a user-defined window. Outliers are avoided by a nonparametric statistical test which compares the relative order

of values within the volume (Daber, 2012). The edge evidence attribute works by searching locally in all directions for line segments where the values on the line differ significantly from the surrounding values. The result is the best evidence of a line passing through that point – evidence of a line gives a high value out and the better the evidence, the higher the output value. Comparison between amplitude contrast and the result of applying the edge evidence algorithm, to that amplitude contrast volume, shows clean linear filaments within the attribute that correspond to the locations of the faults (Figure 4).

Multiple iterations of edge evidence

Multiple applications of the edge evidence attribute have been shown to reduce noise and provide more defined discontinuities within a resultant volume (Daber, 2012). Edge evidence can be adapted to identify edges in horizontal, vertical, and inline/cross line orientations. As a result, the application of combining directional analysis with multiple-edge evidence algorithm passes has the effect of iteratively removing as much noise as possible, while improving the consistency of the filaments within the attribute volume. The initial edge evidence attribute was calculated using the horizontal direction to identify line segments, while the second used the vertical direction. This combination of horizontal and vertical directions to identify potential attribute faults produces a much cleaner attribute (Figure 5). It effectively increases the continuity of the edges found within the data (horizontal orientation) and then sharpens them (vertical direction). Once an appropriately processed edge evidence volume has been generated, it can be passed to the automated fault identification algorithm.

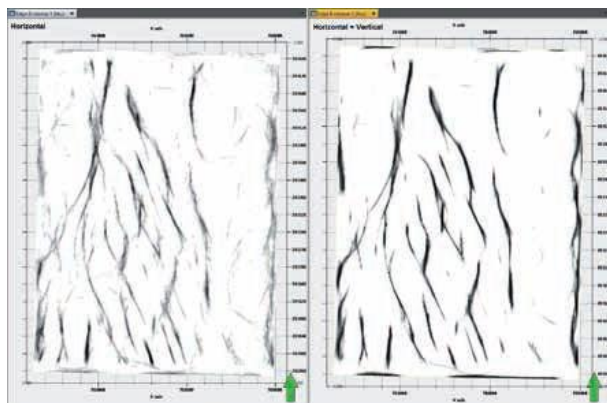


Figure 5 Comparison between single horizontal edge evidence iteration, and combined horizontal and vertical edge evidence.

Evaluating structure using directional extraction

The main tectonic events, such as faulting, are often easy to identify in an amplitude volume; largely due to the way that surveys are designed and acquired. However, the identification of smaller faults or overprinted tectonic events is often poorly illuminated by standard amplitude volumes for reasons already discussed. Identification of these smaller or overprinted events may require alternate illumination from the primary direction. As these smaller features are often the focus for assessing the impact of small faults on reservoir compartmentalization, they are very important to identify. In many cases these small features are not always found to be parallel to the major faulting architecture.

A useful approach is to apply directional analysis that is oblique to the inline illumination direction to help identify

these small features. Without knowing what illumination directions to use, it is usually helpful to generate a range of different directions using the amplitude contrast attribute, which are then passed through the same edge evidence algorithms to highlight the faults. Alternate directional computations of amplitude contrast followed by edge evidence will highlight the differences (Figure 6). The results of the directional analysis clearly show that some features are better identified in oblique orientations to the primary illumination angles (Figure 6). The 90o direction has significantly fewer features identified than the other three extracted directions (0o, 45o and 135o) which suggest that oblique dimension analysis to the dominant tectonic lineament should highlight features more consistently.

Comparison of edge evidence and variance as input

Automated fault extraction usually yields poor results which usually lead interpreters to revert to manual fault interpretation. Typically this is because the quality of the discontinuity information highlighted by the automated fault extraction results is not continuous enough to delineate whole faults. Previous sections have described the problems that classic attributes present in delineating faults: a lack of fault continuity making them very difficult to automatically extract (Figure 7). By comparison, application of the new approach using amplitude contrast and edge evidence shows a much clearer fault fabric throughout the attribute volumes (Figure 8). Automatic fault identification is being achieved using the Ant Tracking algorithm, in the Petrel E&P software platform from Schlumberger. This is designed to assist the identification and extraction of faults in the preconditioned seismic volumes. Once these preconditioned volumes have filtered out all non-relevant data, Ant Tracking can focus on the discontinuities. Named after the behavior of ants in finding their way to and from their colonies by leaving pheromone marker trails for others to follow, the Ant Tracking algorithm works in a similar way by identifying discontinuities in a seismic volume and ‘marking’ them. The identification process then follows these ‘markers’ to generate a fault discontinuity volume (Figures 7 and 8). Ant Tracking results are entirely dependent on the quality of the input data – poorly imaged or processed data will not resolve details effectively.

When edge evidence and variance results are passed through the Ant Tracking process, comparison of the results shows the edge evidence has a significantly improved level of continuity of faults (Figures 7 and 8). Variance attributes demonstrate a similar overall fault pattern, but the fault continuity is far less which creates a significantly poorer result (Figures 7 and 8). It should be pointed out that the settings for the automated fault identification attribute in both the classic and new volumes were the same. This demonstrates a significant improvement in automated fault identification by using the combined amplitude contrast and edge evidence approach.

Incorporating pre-stack seismic data

Analysis of pre-stack data has become increasingly popular in seismic interpretation, where traditional post-stack datasets are not able to delineate some features. This may be due to a number of factors including processing issues, signal-to-noise degradation, and the results of seismic processing. Many of these factors are not controlled by the post-stack data. Allowing interpreters to interrogate the pre-stack data, make custom stacks, modify processing selections, and then interpret it means that they are not bound by default post-stack

processing choices. Investigation of pre-stack gathers, in both offset and angle, show the variability in the degree of features delineated by each of the stacked attributes. Typical analysis of offset gathers often shows that near and far signal bands suffer from a high degree of degradation. Usually the mid-range gathers often have a better consistency, meaning they can resolve more detail (Figures 9, 11, and 12). Many features, such as small faults, are often not resolved by post-stack data so they cannot be incorporated into the seismic interpretation. This has an obvious impact on the understanding of the reservoir compartmentalization and, ultimately, the fluid flow in the reservoir. Interrogation of pre-stack gathers can often highlight these features (Figures 9 and 12) and so improve the overall seismic interpretation.

This article proposes the application of the same fault identification approach to pre-stack data volumes. Here, the automated fault identification is applied to both offset (Figure 9) and angle (Figures 11 and 12) decomposition gathers to assess their applicability for use in conjunction with the results from the post-stack fault identification.

Analysis of offset stacks from pre-stack data was carried out to highlight its differences with angle stacks. The effect of offset analysis on 3D seismic datasets highlights the near-mid, mid, and mid-far channels visually resolves more features with a greater degree of clarity (Figure 9). It is generally accepted that features present in the near and far offsets, in pre-stack data, are often obscured by signal degradation and this can be observed by comparison of the offset stacked panels (Figure 9). Using the results from the offset analysis into automated fault identification shows a number of interesting results when compared to the angle stacks. Results of edge evidence attribute analysis (from amplitude contrast) on the five offset stacks: near, near-mid, mid-, mid-far and far can be seen in Figure 10. Comparison between the angle and offset stacks shows that greater degree of continuous data is highlighted by the angle offsets. This implies that the automated fault extraction algorithms will have problems attempting to extract faults when offset stacks are used as input.

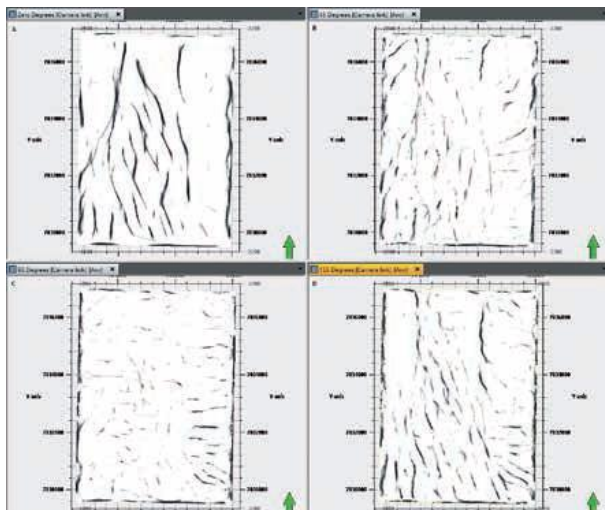


Figure 6 Comparison of edge evidence extraction from directionally computed amplitude contrast attributes (A = 0, B = 45, C = 90, D = 135 degrees)

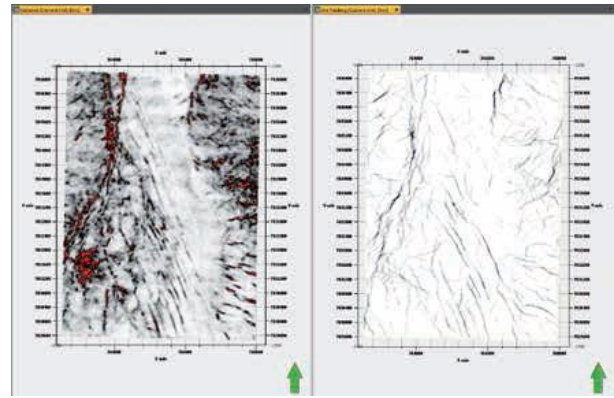


Figure 7 Variance and Ant Tracking volumes showing the low number of clearly delineated faults extracted by the algorithms

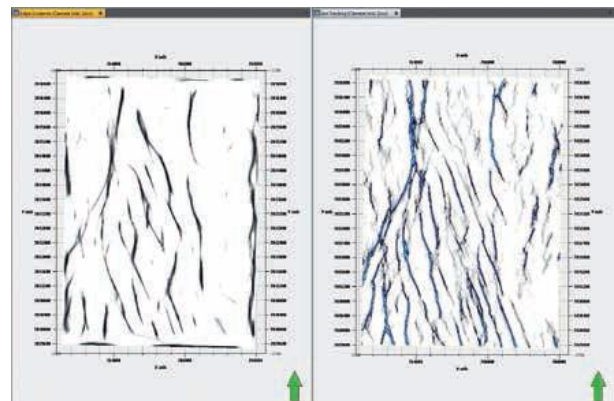


Figure 8 Edge evidence (calculated from amplitude contrast) and the Ant Tracking volume showing clearly delineated fault architecture.

The generation and analysis of different pre-stack angle stacks is proposed to better delineate possible fault discontinuities which are not observed in either the post-stack or offset stack results (Figures 8 and 10). The main idea here is that different angle stacks will highlight features not exposed, or poorly exposed, in other data, such as post-stack cubes. The application of the automated fault identification approach by combining these different angle stacks provides a clearer result of reservoir compartmentalization. A comparison of different angle stacks highlights the varying visible characteristics and features of each (Figures 11 and 12). The mid-range results (between 12o to 42o; Figure 12) visually confirm that features can be delineated with more clarity in comparison to the near and far angles (0–12o and 42–52o); and as a result, the mid-range bands have been selected for use with the automated fault identification.

Comparison between the edge evidence (from amplitude contrast) seismic attribute results on the angle decomposition shows that the five extracted bands share similar features to faulting observed by offset analysis (Figures 10 and 12). However, angle stack features extracted in the near and far bands are less well defined, corresponding with visual analysis of the 3D pre-stack data (Figures 10 and 12). Further comparison of the edge evidence results, from the angle and offset stacks, show the angle decomposition is far better at delineating features in the pre-stack data.

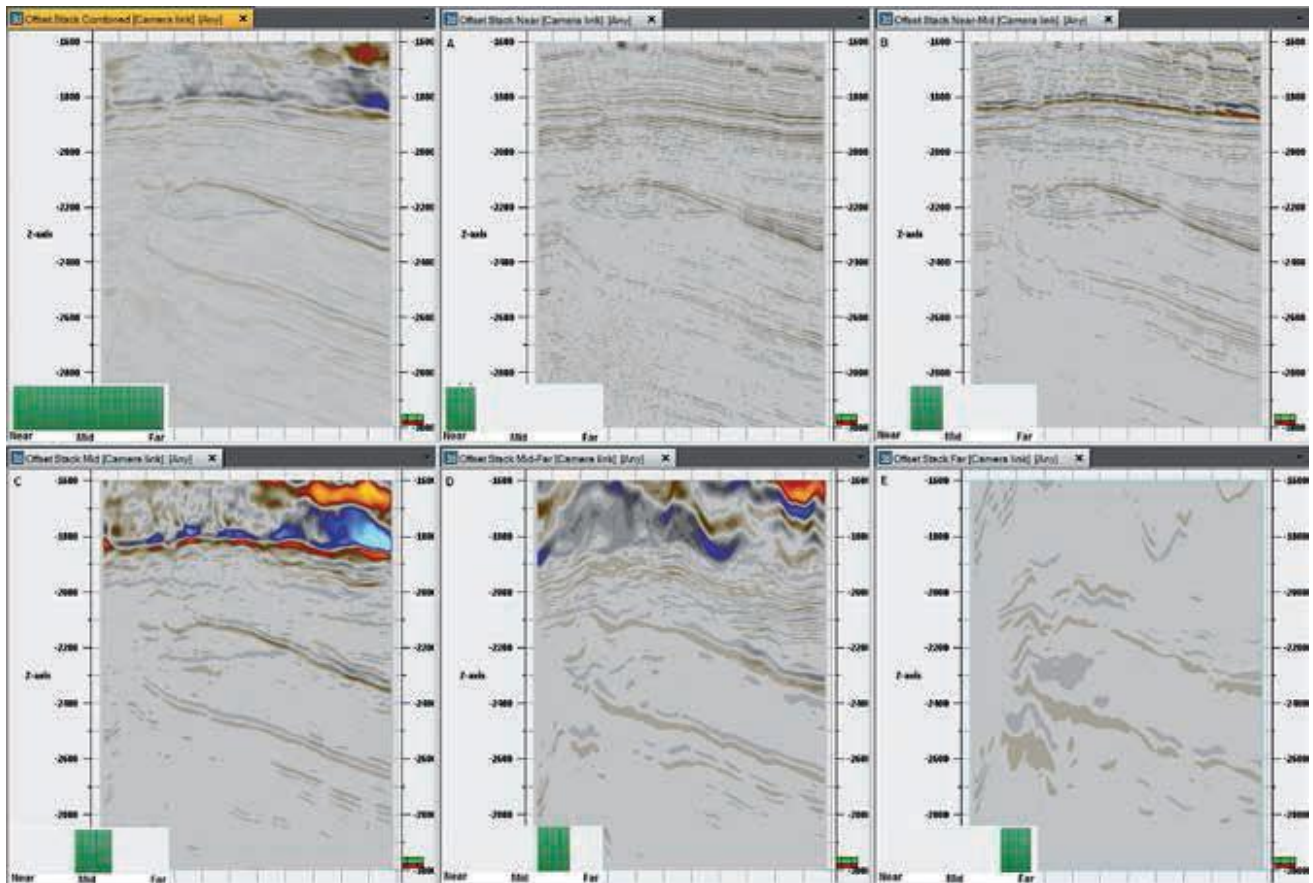


Figure 9 3D Seismic result of offset stacking showing near (a), near-mid (b), mid (c), mid-far (d) and far offsets (e).

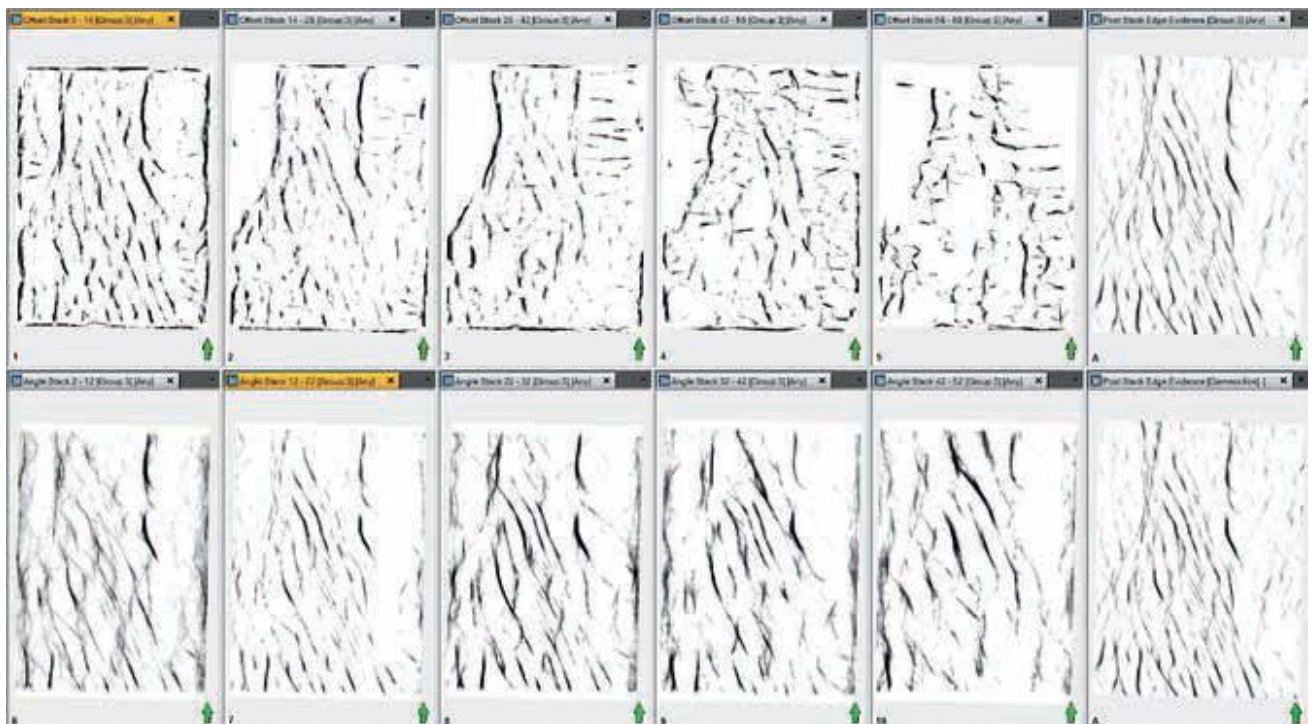


Figure 10 Comparative result of edge evidence attributes. Offset stacking result along the top (1–5) and angle stack result along the base (6–10). Post-stack results (a) are at the end of each row.

When these results are compared with the post-stack results (Figure 10), it can be observed that the angle stack can highlight fault information which post-stack analysis cannot (Figure 8).

Pre-stack fault identification results

Comparison between pre- and post-stack automated fault identification results show a difference between the number and distribution of identified faults (Figure 13). The pre-stack results show a number of faults in the reservoir area which have not been identified by the post-stack analysis (Figure 13a). This implies that pre-stack analysis is able to better delineate data missed by the post-stack. It also suggests that these faults would be missed by automated fault identification in the final interpretation if only post-stack data is used. Comparison of offset and angle stacks in the pre-stack data shows a marked difference where a very limited number of faults have been identified by the offset decomposition in the edge evidence attributes (Figures 10 and 13b, c). This suggests that offset stack data is not an optimal candidate for use with the automated fault identification. Comparing the fault extraction approach with a surface edge detection approach (designed to create a property identifying potential fault location on gridded surfaces), reveals pre-stack result fault locations that match the surface-based result (Figure 14). Some areas in the post-stack seismic data show edge detection results without the corresponding extracted faults. These results demonstrate that pre-stack results do exhibit improved imaging of the fault connections, highlighted by the pre-stack analysis. However, the most complete picture of faults within the seismic data comes from the combination of pre- and post-stack analysis (Figure 13d), meaning the reservoir compartmentalization is better delineated.



Figure 11 Pre-stack panel highlighting the results of the selected angle bands.

Pre-stack fault identification results Comparison between pre- and post-stack automated fault identification results show a difference between the number and distribution of identified faults (Figure 13). The pre-stack results show a number of faults in the reservoir area which have not been identified by the post-stack analysis (Figure 13a). This implies that pre-stack

analysis is able to better delineate data missed by the post-stack. It also suggests that these faults would be missed by automated fault identification in the final interpretation if only post-stack data is used. Comparison of offset and angle stacks in the pre-stack data shows a marked difference where a very limited number of faults have been identified by the offset decomposition in the edge evidence attributes (Figures 10 and 13b, c). This suggests that offset stack data is not an optimal candidate for use with the automated fault identification. Comparing the fault extraction approach with a surface edge detection approach (designed to create a property identifying potential fault location on gridded surfaces), reveals pre-stack result fault locations that match the surface-based result (Figure 14). Some areas in the post-stack seismic data show edge detection results without the corresponding extracted faults. These results demonstrate that pre-stack results do exhibit improved imaging of the fault connections, highlighted by the pre-stack analysis. However, the most complete picture of faults within the seismic data comes from the combination of pre- and post-stack analysis (Figure 13d), meaning the reservoir compartmentalization is better delineated.

CONCLUSIONS

This article demonstrates the benefits of an enhanced automated approach to fault identification and extraction, compared to older seismic attribute methodologies. The new combination of edge evidence from amplitude contrast is significantly better at resolving fault discontinuities in post-stack seismic volumes. Moreover, the addition of pre-stack seismic data further improves these results and allows interpreters to create custom interrogation of the fault distributions within their datasets. Ultimately it highlights that this combined approach yields results which are significantly improved over any individual technique. This new automated reservoir compartmentalization workflow is typical of current developments in digital structural interpretation. It is now possible to interactively reconstruct seismic sections during interpretation using geomechanical principals – for improved geological understanding in complex areas – and automatically extract fault patches to accelerate the interpretation process.

Delineating complex geological structures with confidence or understanding the trends of fault surfaces and fluid flow properties across fault systems are key aspects of modern interpretation and reservoir characterization workflows. Using 3D seismic data, interpreters can spend time understanding the trends of fault surfaces and make correlations from the automatically extracted fault patches instead of creating fault surfaces individually and manually. Detailed edge detection and illumination attribute workflows, including Ant Tracking, can be used for enhanced structural delineation or as input to fracture modelling. Combining edge detection attributes with automatic fault picking significantly reduces conventional interpretation time, while increasing structural awareness and reservoir understanding.

Using geomechanical algorithms to incorporate faults in seismic section reconstruction improves geological understanding. Building structural frameworks digitally increases accuracy and confidence – part of a wider exploration theme to be discussed at the 2014 SIS Global Forum, held in Barcelona on 15–17 April. This biennial industry conference will focus on the future of digitally mitigating E&P risk, using simulation and software technology.

The combination of edge evidence with amplitude contrast – in comparison to structural smoothing followed by variance – provides significantly better automated fault identification. These results are further improved by the inclusion of pre-stack seismic data, especially the use of angle decomposition, which highlights a number of faults that are not resolved by post-stack analysis. The combination of all results and visualization on to an amplitude time slice shows this combined methodology yields far greater detail than any individual approach.

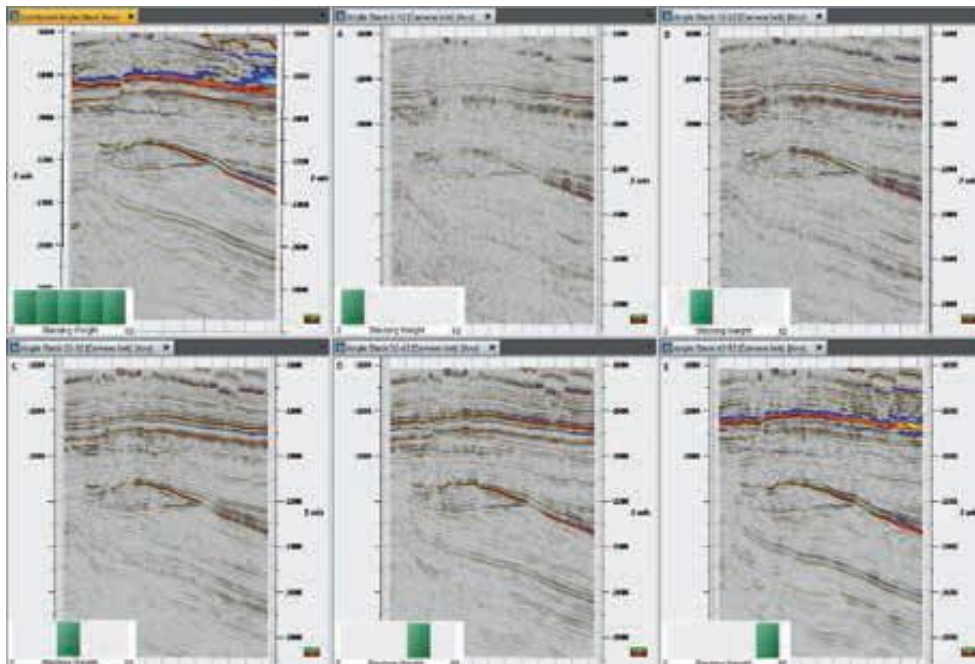


Figure 12 3D Seismic result of angle stacking on the same inline showing 2–12° (a), 12–22° (b), 22–32° (c), 32–42° (d) and 42–52° (e). The results of angle band extraction clearly show the different features highlighted by this analysis and indicate that the mid-range angles provide more features that may be extracted.

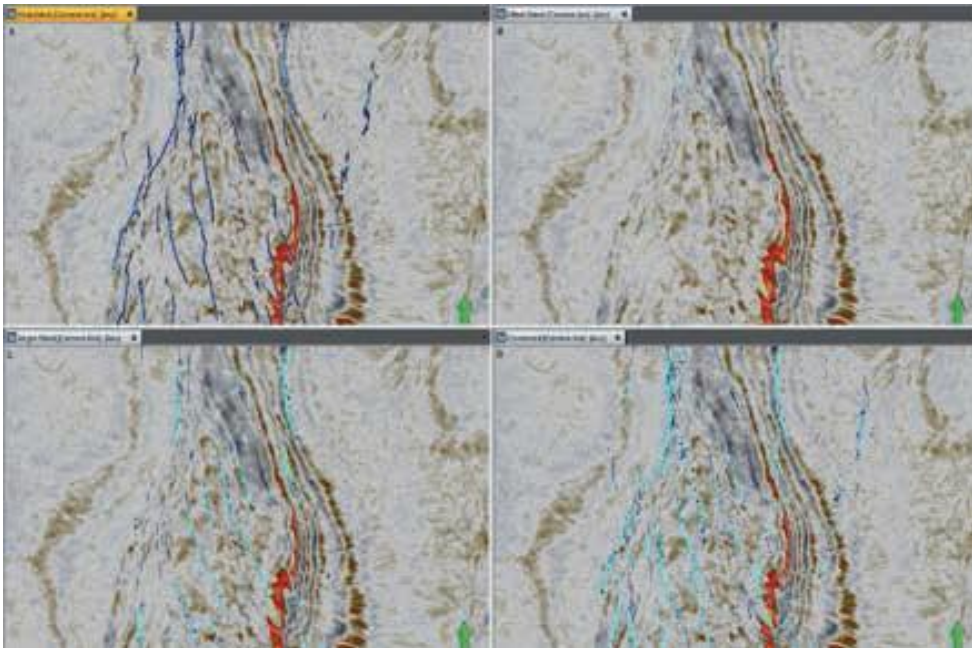


Figure 13 Comparison between post-stack (a), pre-stack angle decomposition (b), pre-stack offset decomposition (c) and combined (pre- and post-stack) results (d).

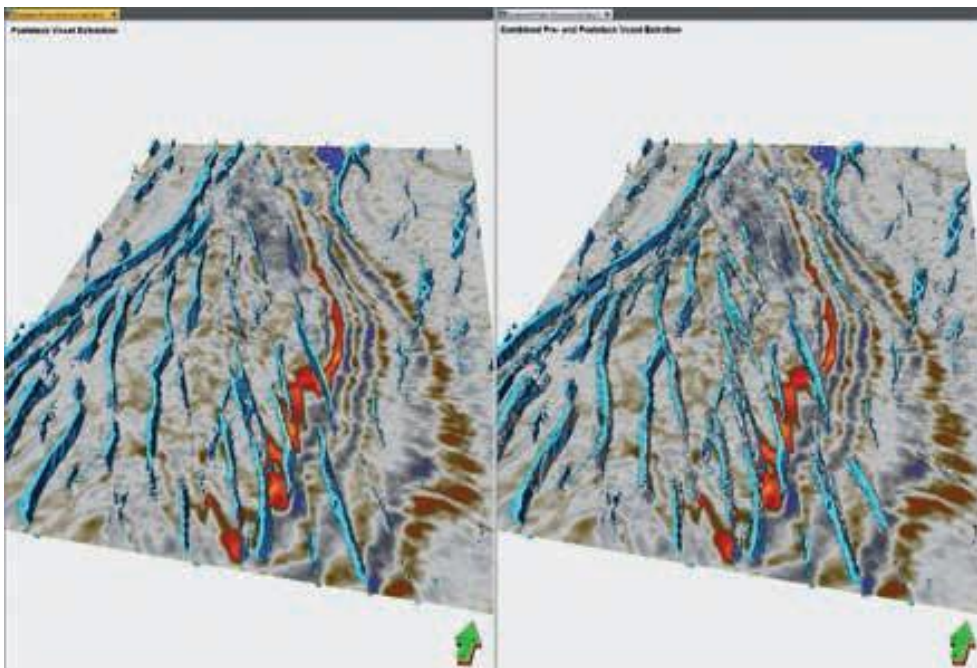


Figure 14 Comparison between post-stack voxel extraction and a combined pre- and post-stack voxel extraction of faults from the Ant Tracking result. The combined results show better fault connections in the central part of the image, indicating that the inclusion of pre-stack data has increased understanding of reservoir compartmentalization.

REFERENCES

- Aqrabi, A.A. and Boe, T.H. [2011] Improved fault segmentation using dip guided and modified Sobel filter. In: SEG Technical Program Expanded Abstracts 2011, 999–1003.
- Aqrabi, A.A., Wolfgang, W., Ralph, D. and Trond, H.B. [2012] Directional guided seismic attributes and their use in assisting structural, stratigraphic and lithological interpretation. In: SEG Technical Program Expanded Abstracts 2012, 1–5.
- Bahorich, M.S. and Farmer, S.L. [1995] 3-D seismic discontinuity for faults and stratigraphic features. *The Leading Edge*, 14, 1053–1058.
- Bahorich, M. and Farmer, S. [1995] The coherence cube. *The Leading Edge*, 14, 1053–1058.
- Cohen, I., and Coifman, R. R. (2002) Local discontinuity measures for 3-D seismic data. *Geophysics*, 67, 1933–1945
- Chopra, S. and Marfurt, K.J. [2008] Emerging and future trends in seismic attributes. *The Leading Edge*, 27, 298–318.
- Daber, R. (ed.) [2012] *Interpreters Guide to Seismic Attributes*. 4th Edition. Schlumberger Information Solutions.
- Duda, R.O. and Hart, P.E. [1972] Use of the Hough transformation to detect lines and curves in pictures. *Comm. ACM*, 15, 11–15.
- Gersztenkorn, A. and Marfurt, K.J. [1996a] Coherence computations with eigenstructure. 58th Conference and Technical Exhibition, EAEG, Extended Abstracts, X031.
- Gersztenkorn, A. and Marfurt, K.J. [1996b] Eigenstructure based coherence computations. 66th Annual International Meeting, SEG, Expanded Abstracts, 328–331.
- Gersztenkorn, A. and Marfurt, K.J. [1999] Eigenstructure-based coherence computations as an aid to 3-D structural and stratigraphic mapping. *Geophysics*, 64, 1468–1479.
- Gonzalez, R.C. and Woods, R.E. [2002] *Digital Image Processing*. 2nd edition, Prentice Hall.
- Hesthammer, J. [1999] Improving seismic data for structural interpretation. *The Leading Edge*, 18, 226–247.
- Iske, A. and Randen, T. (eds) [2005] *Mathematical Methods and Modeling in Hydrocarbon Exploration and Production*. Springer-Verlag.
- Lees, J. A. [1999] Constructing faults from seed picks by voxel tracking. *The Leading Edge*, 18, 338–340.
- Marfurt, K.J., Kirlin, R.L., Farmer, S.L. and Bahorich, M.S. [1998] 3-D seismic attributes using a semblance-based coherency algorithm. *Geophysics*, 63, 1150–1165.
- Marfurt, K.J., Sudhaker, V., Gersztenkorn, A., Crawford, K.D. and Nissen, S.E. [1999] Coherency calculations in the presence of structural dip. *Geophysics*, 64, 104–111.
- Neff, D.B., Grismore, J.R. and Lucas, W.A. [2000] Automated seismic fault detection and picking. US Patent 6 018 498.
- Petersen, S., Randen, I., Sonneland, T. and Steen, O. [2002] Automatic fault extraction using artificial ants. 72nd SEG International Conference, Salt Lake City.
- Pussacq, A. and Aqrabi, A.A. [2012] Enhancing automated fault extraction process with the use of Amplitude Contrast attribute. Petroleum Geoscience Conference & Exhibition, Kuala Lumpur.
- Randen, T., Monsen, E., Signer, C., Abrahamsen, A., Hansen, J.O., Sæter, T., et al. [2000] Three-dimensional texture attributes for seismic data analysis. 70th Annual International Meeting, SEG, Expanded Abstracts, Int. 6.1.
- Radon, J. [1917] Über die Bestimmung von Funktionen durch ihre Integralwerte längs gewisser Mannigfaltigkeiten, *Berichte über die Verhandlungen der Sächsischen Akademie der Wissenschaften*. Reports on the proceedings of the Saxony Academy of Science, 69, 262 – 277.
- Van Bommel, P. and Pepper, R.E.F. [2000] Seismic signal processing method and apparatus for generating a cube of Variance values. U.S. Patent Number 6, 151, 555
- Jing, Z., Yanqing, Z., Zhigang, C. and Li, J. [2007] Detecting boundary of salt dome in seismic data with edge-detection technique. SEG Technical Program Extended Abstract, 26